



Automated identification of impact spatters and fly spots with a residual neural network

Lihong Chen^a, Yaoren Zhu^a, Chuang Ma^b, Zhou Lyu^{a,c,d,*}

^a Criminal Investigation School, Southwest University of Political Science and Law, Chongqing, China

^b School of Software Engineering, Chongqing University of Posts and Telecommunications, Chongqing, China

^c Chongqing Institutions of Higher Education Municipal Key Criminal Technology Laboratory, Chongqing, China

^d Intelligent Research Center of Difficult Homicide Cases Investigation, Southwest University of Political Science and Law, Chongqing, China

ARTICLE INFO

Keywords:

Bloodstain pattern analysis

Impact spatter

Fly spots

Image recognition

Transfer learning

ResNet-18

ABSTRACT

In criminal investigations, distinguishing between impact spatters and fly spots presents a challenge due to their morphological similarities. Traditional methods of bloodstain pattern analysis (BPA) rely significantly on the expertise of professional examiners, which can result in limitations including low identification efficiency, high misjudgment rates, and susceptibility to external disturbances. To enhance the accuracy and scientific rigor of identifying impact spatters and fly spots, this study employed artificial intelligence techniques in image recognition and transfer learning. Two types of bloodstains obtained from simulation experiments were utilized as datasets, and a pre-trained neural network, ResNet-18, was employed for feature extraction. The original fully connected layer was replaced, and a new fully connected layer with a dimensionality of 2 was introduced to fulfil the task requirements. The results demonstrate that the transfer learning network model, based on ResNet-18, achieved a maximum accuracy of 93 % in morphologically identifying impact spatters and fly spots. The objective is to assist crime scene investigators and BPA analysts to identify bloodstains at homicide scenes conveniently, rapidly and accurately, thereby furnishing scientific evidence for scene reconstruction and advancing BPA toward intelligent practices.

1. Introduction

Bloodstain pattern analysis (BPA) employs a multi-disciplinary approach to discern the nature of activities and mechanisms behind bloodstains. BPA draws upon principles from biology, physics, and mathematics to scrutinise and analyze the size, shape, and distribution of bloodstains [1]. This approach has been demonstrated to be an effective tool in the investigation of crime scenes, offering vital clues and robust support for crime scene reconstruction and aiding in case detection during legal proceedings.

Spatter stains are among the most common types of bloodstains found at violent crime scenes [2]. These stains frequently form at the primary crime scene and include subtypes such as spurt, cast-off, and impact spatter [2]. Impact spatter is a type of bloodstain pattern formed by the impact of objects moving at different speeds on blood-stained or blood-containing objects, resulting in blood droplets splattering radially in all directions, which is of great significance for bloodstain analysts to analyze the specific process of the occurrence of the case [3]. These

bloodstains are typically circular or elliptical in shape, and their diameter size is inversely proportional to the force of impact, ranging from 0.01 mm to over 4 mm in diameter [1,3].

In certain homicide scenarios, when an assailant repeatedly strikes the victim's head with a blunt object near a wall, blood droplets may splatter perpendicularly onto the wall, creating overlapping impact spatters [2]. The morphology of these overlapping impact spatters, resulting from multiple impacts, closely resembles the fly spots formed by necrophagous flies regurgitating or defecating onto wall surfaces after licking blood [1,2,4]. On the one hand, fly spots typically have a diameter of 1–2 mm, and exhibit a wide variety of shapes including circular, elliptical, tadpole-like, and teardrop-like shapes [4–6]. These stains may occasionally possess a tail ranging from a few millimeters to less than 20 millimeters in length [4,5]. On the other hand, fly spots may include human blood that has not been fully digested, making it difficult for presumptive blood tests such as Hemastix, Sangur, or Luminol, and DNA typing to differentiate between fly spots and impact spatter [4]. Failure to promptly distinguish between these bloodstain types at a

* Correspondence to: Criminal Investigation School, Southwest University of Political Science and Law, 301 Baosheng Avenue, Chongqing 401120, China.

E-mail address: forensiclzhou@hotmail.com (Z. Lyu).

homicide scene may result in misinterpretation of the facts, potentially leading to misdirection of the investigation [6].

In global forensic practice, disciplines like forensic genetics and forensic toxicology primarily utilize instruments for analysis, and the accuracy of their results is independent of examiner experience. Conversely, BPA demands a high level of expertise from analysts, making it less amenable to widespread application compared to these fields [7]. Those lacking knowledge or with limited training in BPA frequently encounter difficulties in making accurate judgments regarding the morphology and formation mechanisms of specific bloodstains, such as the overlapping impact spatters and fly spots previously mentioned. It is therefore essential to identify bloodstain morphology at crime scenes in a convenient, rapid and accurate manner.

Benecke et al. [4] proposed a method for distinguishing human bloodstains from fly spots based on the calculation of the ratio of tail length to body length. If the ratio is greater than 1, it can be concluded with a high degree of certainty that the observed stain is not human blood. However, Ristenbatt et al. [8] offered a contrasting viewpoint, suggesting that blood droplets striking a surface at an angle could also result in a tail-to-body length ratio greater than 1. They argued that this renders Benecke et al.'s method misleading and potentially dangerous. To address these concerns, Fujikawa et al. [9,10] proposed a method combining the tail-to-body length ratio with the fluorescence of fly spots. Their results revealed that fly defecatory stains could be readily identified by their tailed shape and fluorescence under 465 nm light when viewed with an orange filter. Nevertheless, this method has only been validated for stains formed by *Lucilia sericata* (Meigen, 1826) and *Calliphora vicina* (Robineau-Desvoidy, 1830), and the fluorescence mechanism requires further research. Pelletti et al. [11] utilized scanning electron microscopy (SEM) to observe fly spots on various surfaces. They noted the presence of micro-crystals resembling uric acid, cholesterol, and amorphous crystals on hard, non-absorbent surfaces such as metal and glass. Notably, no red blood cells were observed in the fly spots. It was proposed that SEM analysis could differentiate between fly spots and authentic human bloodstains on hard surfaces. However, this method is only applicable to small, removable samples that fit within the SEM compartment, and is unable to detect bloodstains on concrete floors, stucco walls, or fabric-like absorbent materials.

In addition to the non-destructive testing techniques described above, some scholars have utilized the detection of distinctive components in fly spots to distinguish them from authentic human bloodstains. Rivers et al. [12,13] developed a diagnostic tool (anti-md3 serum) using a pepsin-like enzyme found in the crop of adult *Protophormia terraenovae* (Robineau-Desvoidy, 1830) and in fly regurgitate. The serum exhibited high specificity for bloodstains containing this protein. This result provides evidence that the identification of bloodstain species is feasible by detecting fly digestive enzymes in bloodstains. Nevertheless, it remains unclear whether similar specificity exists for proteases secreted by other necrophagous fly species.

In recent years, the surge in artificial intelligence (AI) image recognition technology has facilitated the completion of numerous identification tasks traditionally reliant on images or morphology, including fingerprint identification [14], bone age assessment [15], pathological section interpretation [16], and cell sorting [17], et al. Moreover, it presents a novel avenue for advancing BPA. Arthur et al. [18] developed an automated bloodstain pattern recognition system utilizing the Fisher quadratic discriminant classifier to accurately distinguish between impact spatter and cast-off bloodstain patterns. When applied to a dataset of impact spatter and cast-off bloodstain patterns on painted and wallpaper substrates, the trained classifier attained an overall error rate of just 2 %, indicating its exceptional accuracy and reliability. 23 bloodstain patterns on a smooth painted surface and 17 patterns on a wallpaper surface were successfully predicted, with only one cast-off bloodstain pattern on the wallpaper misclassified. Zhou et al. [19] collected 2400 images of red ink droplets at varying elevations to simulate bloodstains and applied semi-supervised learning to train a

CaffeNet model. After conducting classification tests on 400 validation samples, the model achieved an accuracy rate of 96.75 %. This study improved the accuracy of bloodstain pattern recognition and introduced a novel methodology for forensic science applications, contributing to crime scene reconstruction and evidence analysis. Liu et al. [20] proposed an automated framework integrating digital image processing and machine learning to classify blood spatter patterns resulting from gunshot and blunt impact at varying distances between the target surface and the blood source. They designed a set of potentially relevant features for classification and applied the random forest algorithm to evaluate feature effectiveness and perform the classification, achieving accuracy rates of 98.81 %, 93.20 %, and 85.96 % at distances of 30 cm, 60 cm, and 120 cm, respectively. This research introduced a mathematical approach to bloodstain pattern analysis, supporting forensic specialists in interpreting complex evidence. The above studies have demonstrated the potential of deep learning in bloodstain pattern recognition while establishing a significant repository of experience and data for future research.

With advances in deep learning techniques, Convolutional Neural Networks (CNNs) have emerged as a breakthrough technology in image recognition. CNNs are feed-forward neural networks that include multi-layer convolutional computation and have a deep structure, demonstrating exceptional performance in image recognition tasks. Classic CNNs models like LeNet [21], AlexNet [22], VGGNet [23], GoogLeNet [24] and ResNet [25] are all open-source deep learning frameworks that have driven the advancement of AI image recognition technology during their respective epochs. In particular, Residual Network (ResNet), building on VGG19 with innovative enhancements and introducing jump connections and residual learning concepts, effectively mitigates issues like vanishing gradients, gradient explosions, and network degradation resulting from the increase in depth of the deep CNNs during training. This improvement dramatically enhances the performance and training speed of CNNs, enabling more effective learning of deeper features and further enhancing image recognition accuracy [25].

This study employed a modified ResNet model to train and evaluate the capacity of AI in recognizing images of impact spatters and fly spots. The objective is to assist crime scene investigators and BPA analysts to identify bloodstains at homicide scenes conveniently, rapidly and accurately, thereby furnishing scientific evidence for scene reconstruction and advancing BPA toward intelligent practices.

2. Material and methods

2.1. Experimental site

The simulation experiment site for impact spatters and the feeding site for necrophilous flies are situated within the BPA experimental field and forensic entomology laboratory of the Chongqing Institutions of Higher Education Municipal Key Criminal Technology Laboratory at Southwest University of Political Science and Law. The activities of the flies at this experimental site remain undisturbed by unrelated individuals, with the exception of scheduled feeding, observation, and documentation.

2.2. Impact spatters simulation experiment

Two wooden screens (300 cm × 4.5 cm × 180 cm) were positioned in the experimental area to replicate an interior wall corner, and a wooden experimental table was placed on the inside of the corner (Fig. 1). A flat polypropylene board was securely affixed at the center of the experimental bench using transparent tape, and the center of the board was 30 cm away from the nearest screen vertically. A multitude of A4 printing paper was affixed to the screen surrounding the experimental bench with pins in an orderly fashion. Fake theatrical blood, made of edible pigments, honey, and sucrose, was used to simulate human blood. A syringe was employed to dispense 1 ml drop of fake theatrical blood

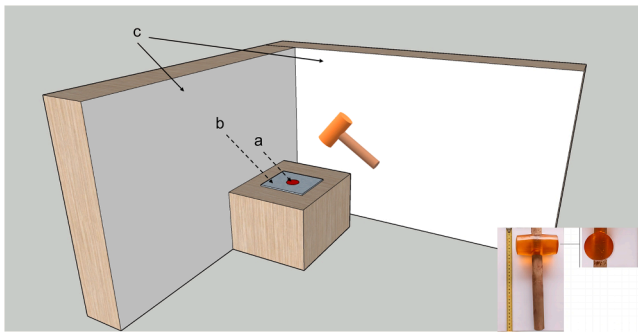


Fig. 1. Impact spatters simulation experimental scene. a. striking area. b. polypropylene plate. c. target surface, using full coverage with a large amount of A4 paper.

onto the center of the polypropylene board. The fake theatrical blood was vertically struck several times with a rubber hammer during each experiment. Subsequently, the A4 papers containing the simulated bloodstains were removed, air-dried and collected. The aforementioned procedure was repeated 20 times, with the A4 printing paper being replaced on the screen each time. Once the initial set of experiments had been completed, the experimental table was relocated, and the distance between the center of the polypropylene board and the screen was adjusted to 50 cm and 100 cm, respectively, for the subsequent repetitions of the experiment.

2.3. Fly spots simulation experiment

A domestic pig carcass (29.6 kg, Fig. 2) was obtained from a local market, slaughtered by the butcher, and subsequently frozen and transported to the laboratory. Once the carcass had been fully thawed, it was placed on plastic trays in the woods on the campus of the Southwest University of Political Science and Law to attract necrophilous flies for egg-laying. The plastic trays were then covered with vermiculite for the larvae to pupate. Upon the departure of the third instar larvae from their food sources for pupation, the fly pupae were harvested from the vermiculite. The most common necrophilous flies in the region during the spring, summer, and fall were filtered from pupae for this study: *Chrysomya megacephala* (Fabricius, 1794), *Chrysomya pinguis* (Walker, 1858), and *Achoetandrus rufifacies* (Macquart, 1843) [26]. In the present study, the authors primarily employed the taxonomic identification criteria from the *Key to the Common Flies of China* [27] to identify the species. The pupae were evenly mixed and divided into two equal portions, which were then placed in two fly-rearing cages. Blank A4 printing papers were spread all over the bottom of the fly-rearing cages (130 × 60 cm × 60 cm, Fig. 3). Once the adult flies had emerged, dishes of milk and fake theatrical blood were placed into the cages. The feed was replenished every two days, while the A4 paper lining the bottom of the cages was collected and replaced until all the flies within the cages



Fig. 2. The domestic pig carcass used to attract flies to lay eggs.



Fig. 3. The fly-rearing cage used in this study.

had died.

2.4. Image acquisition and processing

The A4 papers containing simulated impact spatters and fly spots from the aforementioned experiments were scanned with an Epson L6178 multifunction printer at a resolution of 600 dpi. To prevent misclassification by the modified ResNet model due to color intensity fluctuations caused by adding milk to fake theatrical blood for fly rearing, and to streamline the matrix while improving computational performance, all images were converted to grayscale and stored in TIFF format. This study aims to distinguish between fly spots and impact spatters, which are challenging to identify with the naked eye. Due to the limitations of the employed model, automatic localization of individual stains within the image was not feasible, necessitating manual cropping. In the preliminary analysis, we examined the imaginal body lengths of three fly species selected for the fly spots simulation experiment. The maximum imaginal body length among the specimens did not exceed 12.60 mm. Therefore, stains larger than 12.60 mm in diameter were excluded from the analysis. Additionally, this study manually screened the impact spatters generated in the simulation to exclude those with significant morphological differences from fly spots. When using Adobe Photoshop 2021 to process the collected grayscale bloodstain images, we conducted a series of tests to optimally display the morphological characteristics of each bloodstain. We determined that a 600 × 600 pixels cropping frame was ideal for standardizing image cropping. This step utilized the batch processing function in Adobe Photoshop 2021 to ensure consistency and efficiency in image processing.

2.5. Image recognition

The overall structure of the convolutional neural network is depicted in Fig. 4. ResNet-18 is a neural network model that we utilized to identify various aspects in bloodstain photos. With 17 layers devoted to extracting different details from the images and one final output layer, this network operates similarly to a multi-layered image processing system. By separating distinct "bits of information" from the image, each layer enables the computer to progressively "understand" the material. A "batch normalization" step, which helps stabilize the data as it passes between layers, and many image-processing layers (convolutions) make up each of the "residual blocks" that make up the ResNet-18 model. Furthermore, each block contains "shortcut connections" that allow data to bypass specific layers if necessary. This characteristic keeps information from "vanishing" as it moves through deeper layers, which is a common issue in complicated networks. By the time the information reaches the network's deeper layers, the feature maps (data representations) grow smaller but more sophisticated, allowing the model to make correct classifications. In the last stage, all of the learnt features are combined using a "average pooling" method, and the classification results are obtained via a fully connected output layer with two

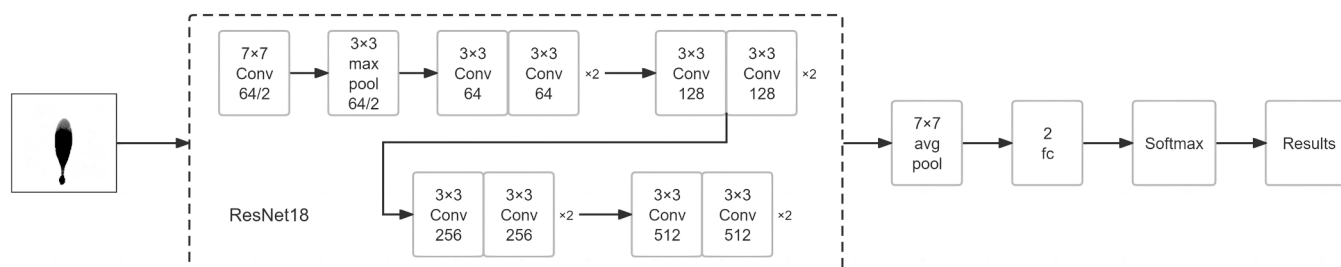


Fig. 4. Modified BPA neural network model based on the ResNet-18 framework. Conv: convolutional layer; fc: fully connected layer.

classification possibilities (dimensions). A "Softmax" function is used at this stage to ensure that the model produces a clear categorization result.

The training and testing process of the model was conducted on a Microsoft Windows 11 operating system. The GPU model employed was the Nvidia RTX-3070 with 8 GB of available video memory. The deep learning programming framework utilized for the experiments was PyTorch. The gradient optimization algorithm employed during training was the Adam algorithm. The loss function used was CrossEntropy Loss, with a fixed learning rate of 0.0001 and a weight decay of 0.0001. The number of epochs was fixed to 50, and the batch size was 128. The preprocessing operations included resizing the images to 250×250 pixels and normalizing the pixel values.

In this study, a total of 14,381 single blood spot grayscale images were collected. A random sampling procedure was employed to partition the preprocessed blood spot grayscale images into a training set and a test set. The training set comprised 13,900 sample images, which is approximately 97 % of the entire dataset. This included 7022 impact spatter images and 6878 fly spot images. The test set comprised 481 sample images, approximately 3 % of the total data, including 224 impact spatter images and 257 fly spot images.

3. Results

3.1. Morphological characteristics of bloodstains images

The bloodstains obtained from the impact spatters simulation experiment (Fig. 5) were observed to be circular, elliptical, and exclamation mark-shaped. The measured diameters of the stains ranged from 0.33 to 12.60 mm, with a relatively concentrated distribution on the

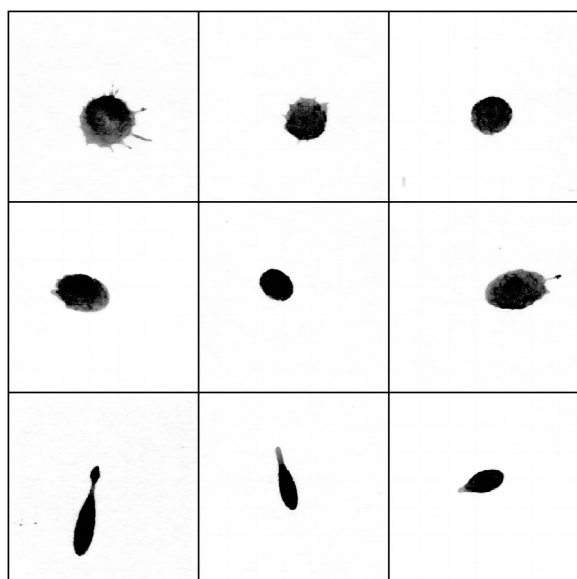


Fig. 5. Laboratory-generated impact spatters.

target surface, radiating clearly from the point of impact to the surrounding area.

In contrast, the bloodstains resulting from the fly spots simulation experiment (Fig. 6) were predominantly circular, elliptical, teardrop-like with tail, exclamation mark-shaped, with some irregular shapes. The measured diameters of the stains ranged from 0.67 to 8.19 mm. The distribution of the stains on the paper surface was relatively disorganized, often exhibiting overlapping between spots.

3.2. ResNet-18 model training results

3.2.1. The loss curve

The training loss represents the average loss of the model on the training set. The loss function, also referred to as the cost function, measures the gap between the model's predicted and true values. Calculated by the model at each iteration based on the training data, the training loss is used to optimize model parameters, guiding updates during the training process. It typically decreases with each epoch, indicating that the model is progressively learning the features of the training data.

The test set, which is not used during training, is typically employed to evaluate the model's generalization ability—specifically, its performance on previously unseen data. The test loss, representing the average

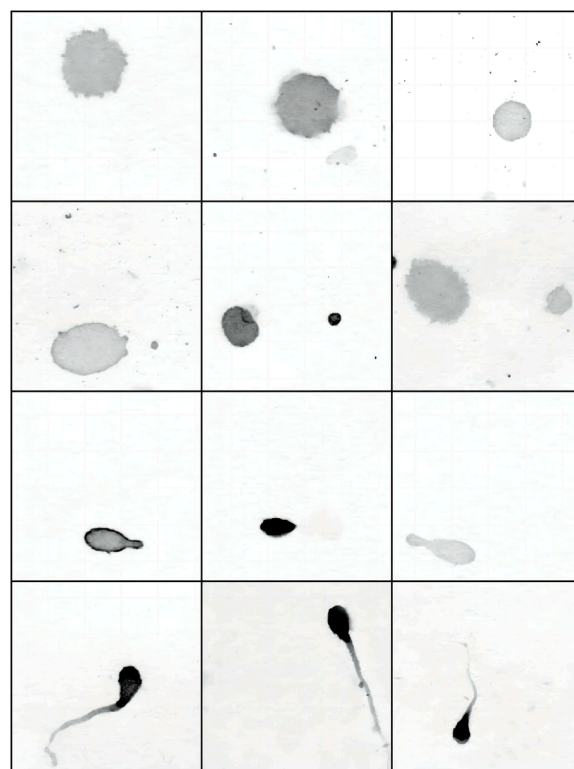


Fig. 6. Laboratory-generated fly spots.

loss on the test set, is used to assess whether the model is overfitting or underfitting. A significantly higher test loss compared to the training loss may indicate that the model performs well on the training data but generalizes poorly on new data, suggesting overfitting. Conversely, if both the training and test losses are high, it may suggest that the model is not adequately learning from the data, indicating potential underfitting.

The numerical curves of training loss and test loss for this study, under the specified parameters, are presented in Fig. 7. The vertical axis represents the model's loss value, while the horizontal axis indicates the number of iterations in the training and test sets. The observed change in loss suggests that both the training set and the test set converged satisfactorily. The loss of the training set demonstrated a gradual decrease with the increase in the number of iterations, while the test set exhibited a similar trend, albeit with a consistently higher loss value compared to the training set.

3.2.2. Recognition accuracy

The numerical curves of training accuracy and test accuracy for this study, under the specified parameters, are presented in Fig. 8. The vertical axis represents the model's accuracy, while the horizontal axis indicates the number of iterations for the training and test sets. The observed change in accuracy indicates that the accuracy of both the training set and the test set increases as the loss decreases. The final accuracy of the training set at convergence is approximately 95 %, while the accuracy of the test set ranges between 0.91 and 0.93.

4. Discussion

Bloodstains serve as crucial physical evidence, often providing significant breakthroughs in challenging cases. They not only verify case facts but also play a pivotal role in reconstructing the crime scene and revealing the truth behind criminal activities. To assist crime scene investigators in distinguishing impact spatter from fly spots accurately and without damaging samples, this study employs a transfer learning model based on ResNet-18 to differentiate the two types of bloodstains. The experimental results demonstrate that the model achieves an overall accuracy rate of 93 %. These findings indicate that the application of residual neural network-based image recognition techniques in BPA is both feasible and highly accurate. This study holds significant scientific value and offers promising applications in BPA. Compared to traditional methods, the AI-based approach minimizes human error and mitigates the risk of misjudgment due to variations in expert experience, thereby enhancing the objectivity and reliability of the results. Furthermore, this technology preserves the integrity of the crime scene by automating the analysis of bloodstain images, eliminating the need for direct contact with the evidence. This innovation not only provides an intelligent solution for BPA but also transforms the conventional, experience-based model into a data-driven approach. Moreover, this technology has substantial practical implications for courtroom forensics. Traditional

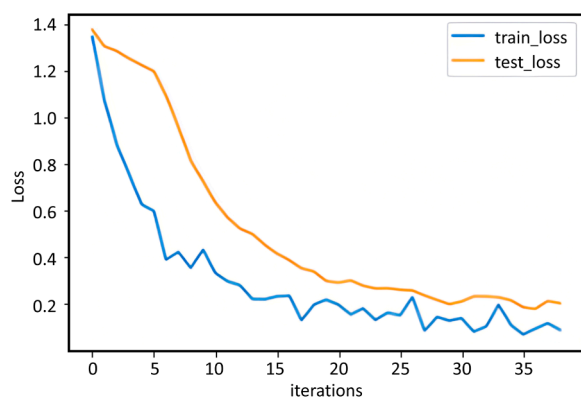


Fig. 7. The iteration loss value curves of the training set and the test set.

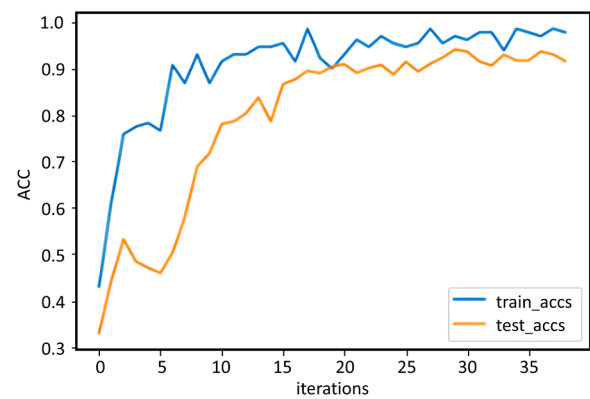


Fig. 8. The iteration accuracy curves of the training set and the test set.

BPA methods often face challenges in terms of accuracy and scientific validity, particularly when expert testimony conflicts with analytical results, which can lead to uncertainty in legal decisions. In contrast, AI technology yields consistent, reproducible analysis results, thereby enhancing the scientific credibility of bloodstain evidence and increasing its acceptance in court, ultimately contributing to the pursuit of justice.

In this study, real human and mammalian blood was not selected for the experiment, primarily due to the bloodstain simulation experiment was scheduled in October–November 2022 in the period of COVID-19 control. During this time, China's regulations on livestock and animal products were further strengthened. According to regional laws and regulations, it was challenging for individuals to obtain fresh blood from food animal slaughterhouses, such as those for pigs, cows, and sheep. Considering that the primary objective of this study was to classify and identify the morphology of impact spatters and fly spots using the ResNet-18 model, Zhou et al. [19] found in their experiment, which utilized a convolutional neural network to analyze morphological images of droplet bloodstains, that the morphological characteristics of bloodstains could be accurately simulated using red ink instead of blood after conducting several tests. Singh et al. [28] also used fake blood made from Awlata dye in drop experiments and observed bloodstain pattern at various heights, confirming the relationship between drop height and the formation of satellite stains and spines. In their study, they suggested that researchers and scientists could use fake blood made from Awlata dye for experimental purposes in future studies. Meanwhile, Byrd et al. [29] and Wang et al. [30] confirmed that adult flies can survive on sucrose and milk, making it feasible to use sucrose-enriched artificial blood combined with milk to feed flies during the fly spots simulation experiment. Due to the presence of pigments and honey in the fake theatrical blood provided to the flies, they may be unable to digest or regurgitate the fake blood as effectively as they do real blood. However, our observations confirmed that adult flies could regurgitate and excrete simultaneously while feeding. In summary, the results of this simulation experiment, using fake theatrical blood instead of real blood, should be sufficient for analysis. Additionally, this study opted to strike blood pools with a blunt object, a scenario more commonly seen in homicide cases, while simulating impact spatters at various distances. This approach more accurately reproduced the distribution and morphological characteristics of the impact spatters.

It is important to note that all bloodstain patterns in this study were formed under controlled laboratory conditions, and only impact spatters and fly spots were modeled. These two types of bloodstains were not present in the same space and did not interact with each other. However, in actual crime scenes involving intentional injuries or homicides, the circumstances can be more complex. Not only is the amount of blood greater, but the variety of bloodstain patterns is also more diverse. The identification process becomes significantly more challenging when different bloodstains mix or overlap. As the model developed in this

study has not yet been applied in real cases, it remains to be determined whether it can be effectively utilized in particularly complex crime scenes. The authors will continue to refine the model in collaboration with local law enforcement.

Additionally, while the transfer learning model based on ResNet-18 employed in this study, excels at feature extraction and classification, its architecture is not equipped to generate spatial location data, such as bounding boxes, for objects. Therefore, the model cannot autonomously identify and localize specific stain regions, particularly for those that are small in size and have low contrast. This limitation makes it challenging for the model to distinguish subtle differences between the stain and the background. To mitigate the impact of background interference on classification, significant manual preprocessing was required prior to stain recognition. These processing steps included but were not limited to, manually screening and cropping individual stains for identification, discarding too large stains, and removing blank areas that interfered with coverage. We also converted the stains to grayscale to prevent interference with the model's identification of features caused by color changes in the fake theatrical blood due to the addition of milk for fly rearing. However, in reality, classification based on bloodstain morphology should also incorporate color information, which requires more exploration in future studies. Nevertheless, the primary focus of this study is to develop a method that can quickly and accurately distinguish between challenging stains in impact spatters and fly spots.

5. Conclusion

In this study, we successfully achieved the effective identification of impact spatters and fly spots by utilizing the transfer learning model based on ResNet-18, developing a new and efficient technological method in forensic bloodstain analysis. This method reduces errors caused by human subjective judgment in the BPA process and enhances the objective credibility of the identification results.

During the study, strict experimental controls and extensive preprocessing steps were conducted to eliminate potential interferences and ensure the quality of data and validity of model training. However, these measures alone are not sufficient for successful application in real crime scene analysis. To facilitate broader use in forensic investigations and assist more analysts in bloodstain analysis, the study must be extended to include a wider range of bloodstain patterns and incorporate bloodstain colors into the morphological identification of these patterns. In future research, we intend to integrate ResNet-18 with an object localization module to enhance the model's ability to distinguish between stains and the background, thereby automating bloodstain detection and localization, and reducing the need for manual preprocessing. Additionally, more realistic and complex environments need to be simulated on various surfaces. Although fake theatrical blood has been demonstrated as suitable for simulating bloodstain experiments in laboratory settings, repeating the study with mammalian blood will be necessary to meet the demands of legal practice, as liquids with differing properties can produce varying shapes and size distributions.

The deep learning technology are assuming an increasingly pivotal role in forensic science in the future. The ongoing advancement of bloodstain analysis techniques is expected to enable fully automated, highly accurate bloodstain evidence analysis, significantly enhancing both the efficiency and precision of forensic investigations. However, challenges remain, including issues related to the explainability and transparency of models, algorithmic biases, and the admissibility of evidence in court. Despite these obstacles, further breakthroughs in forensic bloodstain analysis are likely to provide greater scientific contributions to justice and public safety.

CRediT authorship contribution statement

Lihong Chen: Writing – original draft, Visualization, Investigation, Data curation. **Yaoren Zhu:** Investigation, Data curation. **Chuang Ma:**

Software, Formal analysis. **Zhou Lyu:** Writing – review & editing, Supervision, Resources, Project administration, Methodology, Funding acquisition, Conceptualization.

Declaration of Competing Interest

There is no conflict of interest of this paper.

Acknowledgements

This work was supported by the Science and Technology Fund of Chongqing Education Commission for Young Scientists and Scientific (funding number: KJQN201800305) and key program of Special Projects for Technological Innovation and Application Development of Chongqing Science and Technology Bureau (funding number: CSTB2022TIAD-KPX0109).

Appendix A. Supporting information

Supplementary data associated with this article can be found in the online version at [doi:10.1016/j.forsciint.2024.112354](https://doi.org/10.1016/j.forsciint.2024.112354).

References

- [1] S.H. James, P.E. Kish, T.P. Sutton, *Principles of Bloodstain Pattern Analysis: Theory and Practice*, CRC Press, Boca Raton, 2005.
- [2] T. Bevel, R.M. Gardner, *Bloodstain Pattern Analysis with an Introduction to Crime Scene Reconstruction*, 3rd ed., CRC Press, Boca Raton, 2008.
- [3] L.H. Wan, *Forensic Sceneology*, Peoples Medical Publishing House, Beijing, 2012.
- [4] M. Benecke, L. Barksdale, Distinction of bloodstain patterns from fly artifacts, *Forensic Sci. Int.* 137 (2003) 152–159, <https://doi.org/10.1016/j.forsciint.2003.07.012>.
- [5] A. Durdle, R.A.H. van Oorschot, R.J. Mitchell, The morphology of fecal and regurgitation artifacts deposited by the blow fly *Lucilia cuprina* fed a diet of human blood, *J. Forensic Sci.* 58 (2013) 897–903, <https://doi.org/10.1111/1556-4029.12145>.
- [6] A. Viero, M. Montisci, G. Pelletti, S. Vanin, Crime scene and body alterations caused by arthropods: implications in death investigation, *Int. J. Leg. Med.* 133 (2019) 307–316, <https://doi.org/10.1007/s00414-018-1883-8>.
- [7] A. Bettison, M.N. Krosch, J. Chaseling, K. Wright, Bloodstain pattern analysis: does experience equate to expertise? *J. Forensic Sci.* 66 (2021) 866–878, <https://doi.org/10.1111/1556-4029.14661>.
- [8] R.R. Ristenbatt, P.A. Pizzola, R.C. Shaler, L.N. Sorkin, Commentary on: Mark Benecke and Larry Barksdale, Distinction of bloodstain patterns from fly artifacts, *Forensic Sci. Int.* 137 (2003) 152–159, <https://doi.org/10.1016/j.forsciint.2004.05.012>. *Forensic Sci. Int.* 149 (2005) 293–294.
- [9] A. Fujikawa, L. Barksdale, L.G. Higley, D.O. Carter, Changes in the morphology and presumptive chemistry of impact and pooled bloodstain patterns by *Lucilia sericata* (Meigen) (Diptera: Calliphoridae), *J. Forensic Sci.* 56 (2011) 1315–1318, <https://doi.org/10.1111/j.1556-4029.2011.01800.x>.
- [10] A. Fujikawa, L. Barksdale, D.O. Carter, *Calliphora vicina* (Diptera: Calliphoridae) and their ability to alter the morphology and presumptive chemistry of bloodstain patterns, *J. Forensic Ident.* 59 (2009) 502–512, (<https://www.researchgate.net/publication/272622557>).
- [11] G. Pelletti, D. Martini, L. Ingrà, M.C. Mazzotti, A. Giorgetti, M. Falconi, P. Fais, Morphological characterization using scanning electron microscopy of fly artifacts deposited by *Calliphora vomitoria* (Diptera: Calliphoridae) on household materials, *Int. J. Leg. Med.* 136 (2022) 357–364, <https://doi.org/10.1007/s00414-021-02634-8>.
- [12] D.B. Rivers, G. Acca, M. Fink, R. Brogan, A. Schoeffield, Spatial characterization of proteolytic enzyme activity in the foregut region of the adult necrophagous fly, *Protophormia terraenovae*, *J. Insect Physiol.* 67 (2014) 45–55, <https://doi.org/10.1016/j.jinsphys.2014.06.006>.
- [13] D.B. Rivers, G. Acca, M. Fink, R. Brogan, D. Chen, A. Schoeffield, distinction of fly artifacts from human blood using immunodetection, *J. Forensic Sci.* 63 (2018) 1704–1711, <https://doi.org/10.1111/1556-4029.13756>.
- [14] S. Minocha, K.C. Krishnachalitha, S. Gupta, S.R. Alatba, S.S. Pund, B.S. Alfurhood, A finger print recognition using CNN model, in: 2023 3rd International Conference on Advance Computing and Innovative Technologies in Engineering (ICACITE), IEEE Press, Piscataway, 2023, pp. 1490–1494, <https://doi.org/10.1109/ICACITE57410.2023.10182507>.
- [15] M.S. Sun, Y.H. Ding, Z.Y. Yan, X.M. Su, Application of artificial intelligence in evaluating the bone age image of children, *China Med. Dev.* 36 (2021) 28–32, <https://doi.org/10.3969/j.issn.1674-1633.2021.03.006>.
- [16] S.C. Liu, H.Y. Hu, N.N. Zhu, H. Tang, Application analysis of artificial intelligence in cervical cytology, *Chin. Clin. Oncol.* 28 (2023) 541–544, <https://doi.org/10.3969/j.issn.1009-0460.2023.06.013>.
- [17] Z.D. Diao, L.Y. Kan, Y.L. Zhao, H.B. Yang, J.Y. Song, C. Wang, Y. Liu, F.L. Zhang, T. Xu, R.Z. Chen, Y.T. Ji, X.X. Wang, X.Y. Jing, J. Xu, Y.D. Li, B. Ma, Artificial

- intelligence-assisted automatic and index-based microbial single-cell sorting system for One-Cell-One-Tube, *mLife* 1 (2022) 448–459, <https://doi.org/10.1002/mlf2.12047>.
- [18] R.M. Arthur, J. Hoogenboom, M. Baiker, M.C. Taylor, K.G. de Bruin, An automated approach to the classification of impact spatter and cast-off bloodstain patterns, *Forensic Sci. Int.* 289 (2018) 310–319, <https://doi.org/10.1016/j.forsciint.2018.05.019>.
- [19] B.Y. Zhou, S.H. Gao, An experimental study on analyzing morphological images of droplet bloodstains based on convolutional neural network, *J. People's Public Secur. Univ. China (Sci. Technol.)* 24 (2018) 43–47, <https://doi.org/10.3969/j.issn.1007-1784.2018.01.008>.
- [20] Y. Liu, D. Attinger, K.D. Brabanter, Automatic classification of bloodstain patterns caused by gunshot and blunt impact at various distances, *J. Forensic Sci.* 65 (2020) 729–743, <https://doi.org/10.1111/1556-4029.14262>.
- [21] Y. LeCun, L. Bottou, Y. Bengio, P. Haffner, Gradient-based learning applied to document recognition, *Proc. IEEE* 86 (1998) 2278–2324, <https://doi.org/10.1109/5.726791>.
- [22] A. Krizhevsky, I. Sutskever, G.E. Hinton, ImageNet classification with deep convolutional neural networks, *Commun. ACM* 60 (2017) 84–90, <https://doi.org/10.1145/3065386>.
- [23] K. Simonyan, A. Zisserman, Very deep convolutional networks for large-scale image recognition. 3rd International Conference on Learning Representations, ICLR, Appleton, 2015, pp. 1–14, <https://doi.org/10.48550/arXiv.1409.1556>.
- [24] C. Szegedy, W. Liu, Y. Jia, P. Sermanet, S. Reed, D. Anguelov, D. Erhan, V. Vanhoucke, A. Rabinovich, Going deeper with convolutions, in: 2015 IEEE Conference on Computer Vision and Pattern Recognition (CVPR), IEEE Press, Piscataway, 2015, pp. 1–9, <https://doi.org/10.1109/CVPR.2015.7298594>.
- [25] K. He, X. Zhang, S. Ren, J. Sun, Deep residual learning for image recognition, in: 2016 IEEE Conference on Computer Vision and Pattern Recognition (CVPR), IEEE Press, Piscataway, 2016, pp. 770–778, <https://doi.org/10.1109/CVPR.2016.90>.
- [26] Z. Lv, Insect Succession on Carcasses in Southern Chongqing City and Its Forensic Application, Doctoral dissertation, ChongQing Medical University, 2015 <http://doi.org/10.7666/d.D01119770>.
- [27] Z.D. Fan, *Key to the Common Flies of China*, Science Press, Beijing, 1992.
- [28] P. Singh, N. Gupta, R. Rathi, Blood pattern analysis—a review and new findings, *Egypt. J. Forensic Sci.* 11 (2021) 1–7, <https://doi.org/10.1186/s41935-021-00224-8>.
- [29] J.H. Byrd, J.K. Tomberlin, *Forensic Entomology: The Utility of Arthropods in Legal Investigations*, 3rd ed, CRC Press, Boca Raton, 2019.
- [30] J.G. Wang, F. Zhao, C.L. Lei, Z. Sun, Effects of sugar on *Chrysomya megacephala* (Fabricius) fecundity, *Chin. J. Vector Biol. Control* 16 (2005) 348–350, <https://doi.org/10.3969/j.issn.1003-4692.2005.05.006>.